Journal of Applied Electrochemistry **32**: 305–310, 2002.

Influence of CaF_2 and AlF_3 on the kinetics and mechanism of the Al electrode reaction in cryolite melts with various alumina contents

A. KISZA[1], J. KAŹMIERCZAK[1], J. THONSTAD[2] and J. HIVEŠ[3]
[1]*Faculty of Chemistry, University of Wrocław, 50383 Wrocław, Poland*
[2]*Department of Materials Technology and Electrochemistry, NTNU, 7491 Trondheim, Norway*
[3]*Department of Inorganic Technology, SUT, 81237, Bratislava, Slovakia*

Received 13 July 2001; accepted in revised form 13 November 2001

Key words: alumina, aluminium electrolysis, aluminium trifluoride, calcium difluoride, double layer capacitance

Abstract

Electrochemical techniques were used to study the kinetics and mechanism of the aluminium electrode reaction in two cryolite-based melts containing cryolite with either 11 wt % AlF_3 or 5 wt % CaF_2 additions and variable alumina contents at 1000 °C. A three step electrode process was observed in both melts, comprising a preceding chemical reaction followed by two charge transfer steps. The exchange current density of the cathodic reaction was found to be dependent on the concentration of aluminium fluoride. By a combination of electrochemical impedance spectroscopy (EIS) and galvanostatic relaxation methods (GRM), the exchange current density of the first (slower) charge transfer step, the Warburg diffusion impedance, the double layer capacitance of the aluminium electrode and the rate of the preceding chemical step, were evaluated in the range of 2–8 wt % alumina. The role of the two additives, AlF_3 and CaF_2, was evaluated.

List of symbols

A	electrode area (cm^2)
A, B, C	coefficients of Equation 5
C_{dl}	double layer capacitance (F)
c	concentration (mol cm^{-3})
D_i	diffusion coefficient of species i (cm^2 s^{-1})
F	faradaic constant (C mol^{-1})
j_0	exchange current density (A cm^{-2})
L_1, L_2	high frequency and low frequency inductance (H)
L_{out}	outer inductance (H)
R_{el}	electrolyte resistance (Ω)
n	number of electrons (dimensionless)
R	molar gas constant (J $mol^{-1}K^{-1}$)
R_{ct}	charge transfer resistance (Ω)
T	temperature (K)
t	time (s)
Z_W	Warburg impedance (Ω $s^{-1/2}$)
α, β	coefficients of Equation 5 ($s^{-1/2}$)
γ	coefficient of Equation 5 (s^{-1})
η	overpotential (V)

1. Introduction

The mechanism and kinetics of the aluminium electrode reaction in aluminium electrolysis is highly influenced by the composition, the ionic structure of the molten electrolyte and the double layer structure. The structure of cryolite melts is rather complex. In our previous papers [1–3] we used the classical model for cryolite dissociation, according to which the dissociation reaction can be represented by the following equations:

$$Na_3AlF_6 = 3\,Na^+ + AlF_6^{3-} \quad (1)$$

$$AlF_6^{3-} = AlF_4^- + 2\,F^- \quad (2)$$

where the degree of dissociation of the cryolite anion in pure cryolite (Equation 1) is approximately 0.25, increasing with decreasing NaF/AlF_3 molar ratio [4]. This dissociation model is not universally accepted, as some authors claim that the AlF_5^{2-} ion is present [4–7]. Our previous measurements were performed mainly in cryolite melts with varying concentration of alumina and in industrial type melts also containing 11 wt % AlF_3 and 5 wt % CaF_2. However, the influence of the two main additives (AlF_3 and CaF_2) has not yet been established.

The solubility of alumina in cryolite amounts to about 24 mol % at around 1000 °C, and it decreases appreciably by addition of other fluorides, including AlF_3 and CaF_2. In an alumina-saturated cryolite melt a large fraction of the aluminium fluoride complexes are present

in the form of oxyfluoride anions. The dissolved alumina forms binuclear oxyfluoride complexes of the type $Al_2OF_6^{2-}$, $Al_2O_2F_4^{2-}$ [4], and also complexes with higher coordination numbers of fluoride anions have been suggested, for example, $Al_2OF_{10}^{6-}$ [8] and $Al_2OF_8^{4-}$ [9]. The latter oxyfluoride complexes are in equilibrium with the less coordinated anions. For example,

$$Al_2OF_{10}^{6-} = Al_2OF_6^{2-} + 4\,F^- \tag{3}$$

Addition of the two main additives, AlF_3 and CaF_2, may exert an influence on the above equilibria (Equations 2 and 3) and on the charge transfer steps, which may also lead to a change in the rate of the cathode reaction compared with pure cryolite–alumina melts.

In this work the kinetics and mechanism of the cathodic reaction was studied in two types of cryolite-based melts. The first melt was composed of cryolite and 11 wt % AlF_3 with 0, 2, 4, 6 and 8 wt % Al_2O_3, respectively, whereas the second was composed of cryolite with 5 wt % CaF_2 and 0, 2, 4, 6 and 8 wt % Al_2O_3.

It has to be emphasized, that the reactant of the cathodic reaction in aluminium electrolysis is the aluminium tetrafluoride complex anion AlF_4^-, which has to undergo total dissociation reaction before aluminium is deposited. Although the enhanced dissociation of weak electrolytes under the influence of a strong electric field has been known from the beginning of the 20th century, this fact was never used in the interpretation of the kinetic results in molten salts electrode reactions. A strong electric field may be created at the electrode surface by the primary solvation shell (compact Helmholtz layer), which is different in the two melts studied.

2. Method of measurements

Electrode reactions on metallic electrodes in their pure molten salts are generally very fast because of the high temperature of the melt and high concentrations of the reacting ions. For these reasons such electrode reactions are seen by most classical electroanalytical methods as being reversible. They are characterized by a high exchange current density. High energy electrode reactions are inductive, which means that the equivalent circuit that can be used to represent such an electrode reaction contains inductance. The cathodic reaction in aluminium electrolysis is a high-energy, very inductive electrode reaction [10, 11], which implies that its exchange current density is larger than 0.1 A cm^{-2}. Such an electrode can be represented by the equivalent circuit presented in Figure 1(a). In the case of an electrode process with two charge transfer reactions, the equivalent circuit presented in Figure 1(b) should be used, as described in our earlier paper [1].

For the evaluation of the exchange current density of a high energy electrode a combination of electrochemical impedance spectroscopy (EIS) [12, 13] and the

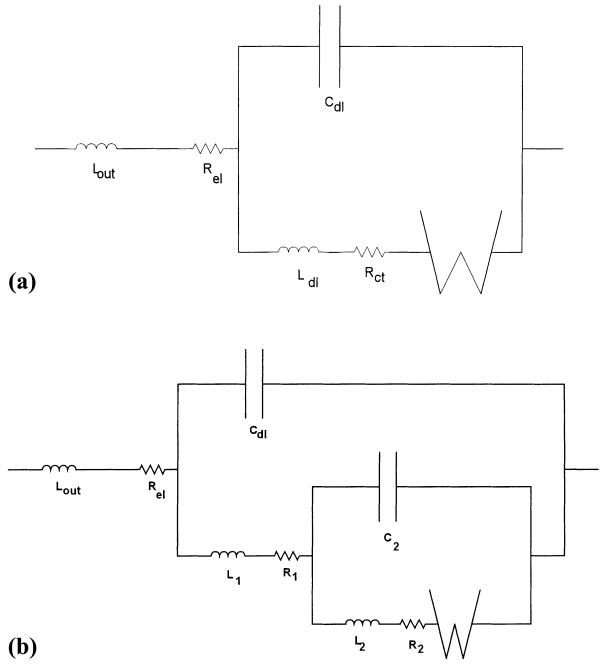

Fig. 1. Equivalent circuits (see text).

galvanostatic relaxation method (GRM) [10, 11] can be used. The charge transfer resistance is obtained from the equation derived in [11],

$$R_{ct} = L_2(\alpha\beta + \gamma) \tag{4}$$

where the three time domain parameters α, β and γ are obtained by the NLLSFit (nonlinear least squares fit) of the galvanostatic relaxation curve described by the Equation 5,

$$\eta(t) = A\exp(\alpha^2 t)\mathrm{erfc}(\alpha\sqrt{t}) + B\exp(\beta^2 t)\mathrm{erfc}(\beta\sqrt{t}) + C\exp(-\gamma t) \tag{5}$$

and the inductance L_2 from the NLLSFit of the low frequency part of the impedance spectra.

The exchange current density j_0 is then obtained from the charge transfer resistance R_{ct} by the equation

$$j_0 = \frac{RT}{nFAR_{ct}} \tag{6}$$

where A is the electrode surface area, the other terms having their usual meaning.

The Warburg diffusion impedance Z_W can be evaluated either directly from the NLLSFit of the recorded impedance spectra, using the equivalent circuits presented in Figure 1, or by using a combination of the EIS and GRM methods [10, 11] by the equation,

$$Z_W = L_2(\alpha + \beta)\gamma \tag{7}$$

It is important to note that the time domain parameters α, β and γ of Equations 4 and 7 should be evaluated from the relaxation curves recorded in the same mea-

suring cell as the low frequency inductance L_2, that is known from a separate EIS measurement in the same experiment.

3. Experimental detail

3.1. *Materials*

Crystals of hand-picked Greenland cryolite were used without further purification. The γ-Al_2O_3 (Fluka), AlF_3 and CaF_2 were of analytical grade. All three aluminium electrodes (working, reference and counter electrodes) were made up of super purity aluminium (99.99% Al).

3.2. *Apparatus and experimental procedure*

The experimental cell for the study of the cathodic reaction that was used for both relaxation and impedance measurements, is presented in Figure 2. The aluminium working electrode and the reference electrode were identical, with an aluminium surface area of 0.14 cm^2. A liquid aluminium pool in BN was used as a counter electrode. The measuring cell was kept in dry argon in an electrically heated furnace with temperature control to ± 0.2 K. The cell was equilibrated at a given temperature for at least 1 h. For the GRM measurements a constant current pulse between the working and the auxiliary electrodes was supplied by a PAR (model 173) potentiostat–galvanostat with a PAR (model 175) universal programmer. The duration of the current pulse was always 0.1 ms. The current was chosen in such a way ($\sim$150 mA) that the resulting overpotential perturbation at zero time did not exceed 30–70 mV. The relaxation of the overpotential of the working electrode (versus the reference electrode in the same melt) was recorded on a LeCroy LS140 Scope Station. The faradaic impedance spectra were recorded using a computer-controlled Solartron 1260 phase-gain analyser with a Solartron 1286 interface, and the measurements were controlled by a PC through a GPIB connection by means of original Solartron measuring software. The impedance measurements of the cathodic reaction were performed at the equilibrium potential of the aluminium electrode, that is, no d.c. current was passed.

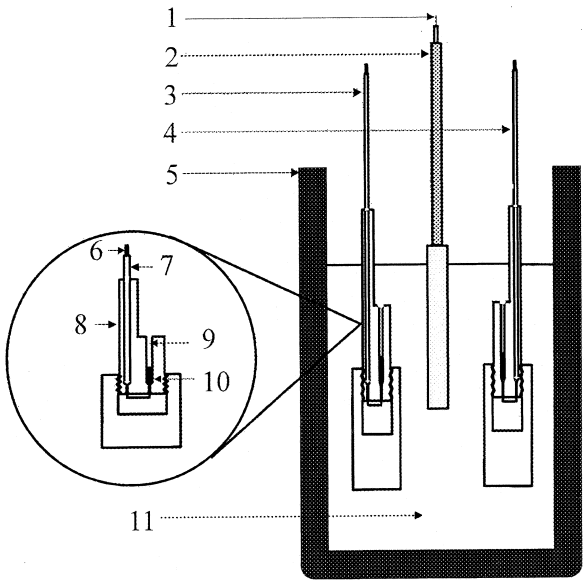

Fig. 2. Experimental cell. (1) molybdenum wire, (2) counter electrode (Al in BN), (3) working electrode (Al in BN), (4) reference electrode (Al in BN), (5) graphite crucible, (6) molybdenum wire, (7) alumina tube, (8) BN body, (9) connecting hole filled with the melt, (10) liquid, and (11) melt.

4. Results and discussion

4.1. *Exchange current density*

Based on our previous studies the mechanism of the cathodic reaction in cryolite melts may be written in two change transfer steps:
(i) *a low frequency charge transfer*

$$AlF_4^- + 2\,e^- = AlF_2^- + 2\,F^- \tag{8}$$

(ii) *high frequency charge transfer*

$$AlF_2^- + e^- = Al + 2\,F^- \tag{9}$$

The steps in this mechanism have considerably different rates. The first charge transfer step (Equation 8) involves diffusion of the tetrafluoride AlF_4^- anion toward the cathode, its partial dissociation and the transfer of two electrons. We shall refer to that step as a low frequency step, because charge transfer with diffusion is observed in the low frequency part of the impedance spectrum. It is slower as compared to the subsequent step (Equation 9), in which the intermediate reactant AlF_2^- is at the reaction site, and it involves only one electron transfer. We shall refer to the second charge transfer step (Equation 9) as a high frequency step, since such processes are observed in the high frequency part of the impedance spectrum. The exchange current density of the high frequency step, being of the order of 20 A cm^{-2}, was found to be slightly dependent on the melt composition. Since it is larger than the cathodic current density used in the industrial process, which is in the region of 0.5 A cm^{-2}, it does not produce any significant overpotential.

In this paper we shall evaluate only the exchange current density of the low frequency step (Equation 8), as having a possible influence upon the value of the cathodic overpotential. A typical relaxation curve is presented in Figure 3, recorded in the millisecond time range after galvanostatic perturbation of the working aluminium electrode in a melt containing Na_3AlF_6, 5 wt % CaF_2 and 8 wt % Al_2O_3. A nonlinear least squares fit (NLLSFit) of such a curve described by Equation 5, yields the time domain parameters α, β and

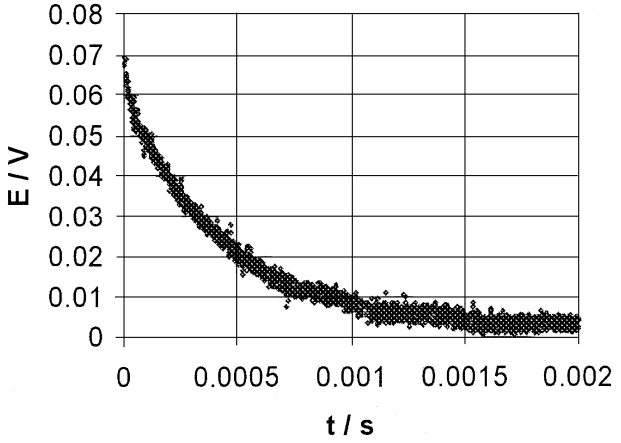

Fig. 3. Relaxation curve in the millisecond time range in a melt containing Na_3AlF_6, 5 wt % CaF_2 and 8 wt % of Al_2O_3 after perturbation.

γ which can be used to evaluate the charge transfer resistance by Equation 4.

The value of the low frequency double layer inductance (L_2), necessary for the evaluation of the charge transfer resistance, was obtained from a NLLSFit of the recorded impedance spectra in the frequency range from 100 Hz to 10 000 Hz, by the use of the Boucamp program [14]. An example of such an impedance spectrum for a cryolite melt containing 11 wt % AlF_3 and 4 wt % Al_2O_3 (markers) together with its NLLSFit (solid line), is presented in Figure 4.

The exchange current density as a function of the alumina content is presented in Figure 5. In addition to the melts studied here (with the content of AlF_3 or CaF_2) also data for an industrial type melt, published earlier [3], are shown. This graph is to some extent remarkable. The highest exchange current density is observed for the melt containing CaF_2, whereas the addition of AlF_3 lowers the rate of the cathodic reaction. The industrial melt containing both additives at the same concentrations, has an intermediate exchange current density [3]. The addition of AlF_3 lowers the rate by, presumably, the influence of that species on

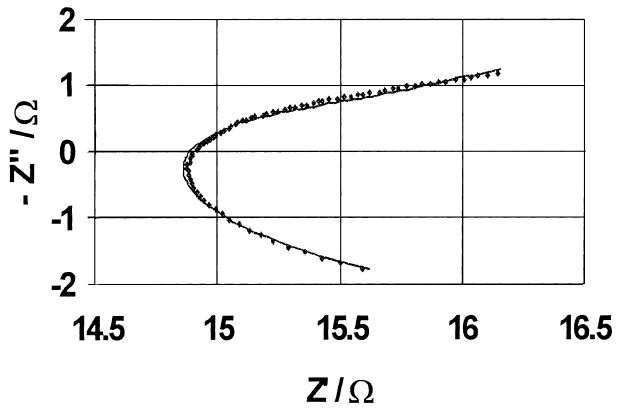

Fig. 4. Impedance spectrum of the aluminium electrode in a melt containing Na_3AlF_6, 11 wt % AlF_3 and 4 wt % Al_2O_3. Plots: experimental values, line: NLLSFit.

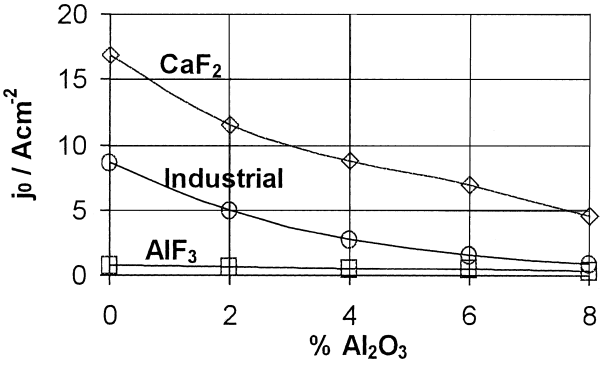

Fig. 5. Exchange current density of the aluminium electrode in melts studied at various alumina content.

the formation of the primary solvation shell on the cathode surface.

All exchange current densities decrease with increasing alumina content. The reason for this may be simply a decrease in the AlF_4^- concentration due to the consumption of this ion by the alumina dissolution reactions. For example,

$$Al_2O_3 + 4\,AlF_4^- + 2\,F^- = 3\,Al_2OF_6^{2-} \qquad (10)$$

$$Al_2O_3 + AlF_4^- + 2F^- = \frac{3}{2}\,Al_2O_2F_4^{2-} \qquad (11)$$

4.2. *Diffusion impedance*

The fit of the experimentally recorded impedance spectra according to the equivalent circuit presented in Figure 1(a) also gives the Warburg diffusion impedance. Such an evaluated value of the diffusion impedance contains contributions from both oxidized (AlF_4^-) and reduced (AlF_2^-) ionic species and represents their diffusion through the melt and in the reaction layer at the cathode surface. Similarly this value is obtained by a combination of the EIS and GRM methods by the use of Equation 7. In both cases the total Warburg diffusion impedance is obtained. The value of the Warburg diffusion impedance, Z_W, obtained from the NLLSfit of the impedance spectra by the equivalent circuit approach was the same as the value obtained by the evaluation of the impedance by a combination of the EIS and GRM methods. The dependence of the Warburg diffusion impedance on the alumina content in the two melts under study is presented in Figure 6.

It is seen in Figure 6 that, in concordance with the kinetic results, the Warburg diffusion impedance, related to the diffusion of the AlF_4^- anion, is higher in the melt containing 11 wt % AlF_3. The main reason for the higher diffusion impedance in the melt containing 11 wt % AlF_3, is the same as for the decreases in the exchange current density in this melt and the explanation has been found in the structure of the primary solvation shell at the aluminium cathode as described in the double layer capacitance study.

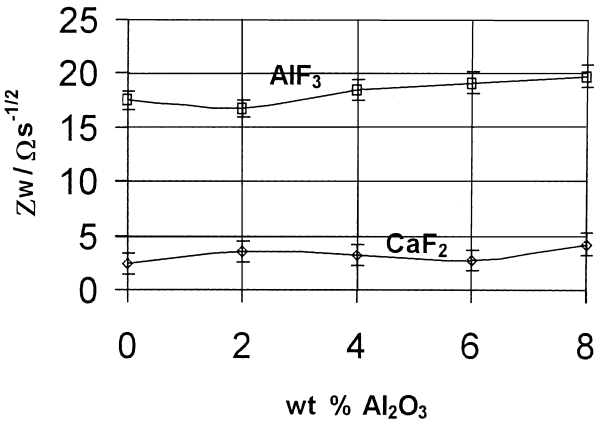

Fig. 6. The Warburg diffusion impedance in the melts studied at various alumina content.

4.3. *Double layer capacitance*

The method of evaluation of the double layer capacitance of high energy electrodes is described in another paper [15], and only the results of such an evaluation for the aluminium electrode in the two melts studied will be given here. It is presented graphically in Figure 7. As shown in the previous paper [15], the value of the double layer capacitance of a reversible electrode depends on the structure of the melt at the interface, and decreases with increasing exchange current density. A decrease in the double layer capacitance with increasing exchange current density is clearly observed in both melts (Figure 7(a)). There are two considerable differences in the double layer structure of the aluminium electrode in the two melts studied. In cryolite melt with 5 wt % of CaF_2, the primary solvation shell is composed of free fluoride anions, which are rather small, as compared to large AlF_4^- anionic species. No adsorption of a neutral species (AlF_3) was found. The electric field intensity at the inner Helmholtz plane in the melt with 5 wt % of CaF_2 is thus large ($\sim 2.5 \times 10^9$ V cm^{-1}). The main constituent of the primary solvation shell on the liquid aluminium electrode in the cryolite melt with 11 wt % of AlF_3 is a large AlF_4^- anion. To reproduce the values of the double layer capacitance in that melt, an adsorption of a neutral species (AlF_3) had to be assumed in the range from 10 to 20% of the active aluminium electrode area. The electric field intensity at the inner Helmholtz plane in this melt is thus smaller ($\sim 4.8 \times 10^8$ V cm^{-1}). The rate of dissociation of the AlF_4^- anion in the melt with 5 wt % of CaF_2, due to much higher field intensity is much higher, which is the main reason, why the exchange current density in that melt is the largest. The rate of dissociation of the AlF_4^- anion in the melt with 11 wt % of AlF_3, due to lower electric field intensity is thus smaller, which reduces the exchange current density. As mentioned above the second reason for exchange current density decrease in the melt with 11 wt % of AlF_3, is the adsorption of about 20% of the electrode area by a neutral species.

The analysis of the impedance spectra by the theory of the impedance of an electrode reaction preceded by a chemical step, should reveal the differences in the rates of the preceding chemical steps in these two melts.

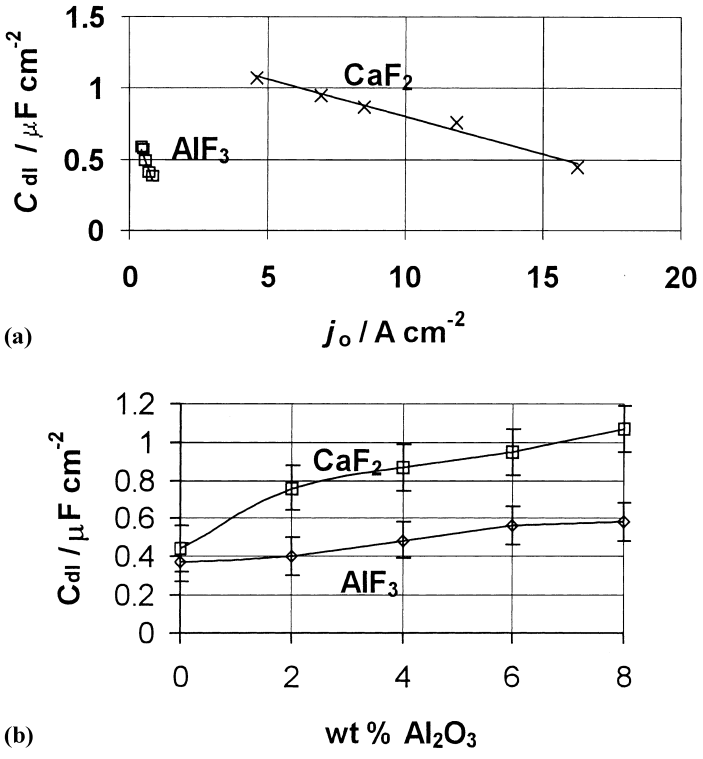

Fig. 7. Double layer capacitance of the aluminium electrode in the melts studied: (a) against exchange current density, and (b) at various alumina content.

4.4. *Rate of the preceding chemical step*

The low frequency charge transfer step given by Equation 8, must contain the dissolvation step, which can be written in several ways. For example,

$$AlF_4^- \underset{k_1}{\overset{k_2}{\rightleftharpoons}} AlF_2^+ + 2\,F^- \tag{12}$$

$$AlF_2^+ + 2\,e^- = AlF_2^- \tag{13}$$

The theory is given elsewhere [12] and the evaluation can be found in our earlier paper [16]. The important results of the evaluation is the sum of the two rate constants k_1 and k_2:

$$k = k_1 + k_2 \tag{14}$$

which appeared to be 105 000 s^{-1} in the melt with 5 wt % of CaF_2 but only 370 s^{-1} in the melt with 11 wt % of AlF_3.

It seems that the large difference in the exchange current density in the cathodic reaction in the two melts studied, is a result of the compact Helmholtz layer structure.

References

1. J. Thonstad, A. Kisza and J. Kaźmierczak, *J. Appl. Electrochem.* **26** (1996) 102.
2. A. Kisza, J. Thonstad, J. Kaźmierczak, T. Eidet and J. Hives, Proceedings of 'Molten Salt Chemistry and Technology', Dresden, Trans. Tech. Publ. Switzerland, *Molten Salt Forum* **5–6** (1998) 263.
3. A. Kisza, J. Kaźmierczak, J. Thonstad, T. Eidet and J. Hives, *Light Metals* **1999**, 423.
4. K. Grjotheim, C. Krohn, M. Malinovsky, K. Matiasovsky and J. Thonstad, '*Aluminium Electrolysis, Fundamentals of the Hall–Heroult Process*', 2nd edn (Aluminium Verlag, Düsseldorf, 1982).
5. F. Bouyer, G. Picard and J.J. Legendre, *Intern. J. Quant. Chem.* **52** (1994) 927.
6. E. Robert, V. Lacassagne, C. Bessada, D. Massiot, B. Gilbert and J-P. Coutures, *Inorg. Chem.* **38** (1999) 214.
7. B. Gilbert and T. Materne, *Appl. Spectrosc.* **44** (1990) 299.
8. A. Sterten, *Electrochim. Acta* **25** (1980) 1673.
9. H. Kvande, *Light Metals* **1986**, 451.
10. A. Kisza, *Polish J. Chem.* **67** (1993) 885.
11. A. Kisza, *Polish J. Chem.* **68** (1994) 613.
12. J.A. Bard and R.L. Faulkner, '*Electrochemical Methods, Fundamentals and Applications*', (J. Wiley & Sons, New York, 1980).
13. J.R. Mcdonald, '*Impedance Spectroscopy*' (J. Wiley & Sons, New York, 1987).
14. B. Boucamp, '*Equivalent Circuit*', (University of Twente, Holland, 1988/89).
15. A. Kisza, *J. Electroanal. Chem.*, in press.
16. A. Kisza, J. Dzielendziak and J. Kaźmierczak, Proceedings of the 11th international symposium on 'Molten Salts', JES, **98–11** (1998) 398.